FRONT-FLASH THERMAL IMAGING CHARACTERIZATION OF CONTINUOUS FIBER CERAMIC COMPOSITES

C. Deemer, J. G. Sun, W. A. Ellingson, and S. Short†

Argonne National Laboratory
Argonne, IL 60439

†Northern Illinois University
DeKalb, IL 60115

ABSTRACT

Infrared thermal imaging has become increasingly popular as a nondestructive evaluation method for characterizing materials and detecting defects. One technique, which was utilized in this study, is front-flash thermal imaging. We have developed a thermal imaging system that uses this technique to characterize advanced material systems, including continuous fiber ceramic composite (CFCC) components. In a front-flash test, pulsed heat energy is applied to the surface of a sample, and decay of the surface temperature is then measured by the thermal imaging system. CFCC samples with drilled flat-bottom holes at the back surface (to serve as "flaws") were examined. The surface-temperature/time relationship was analyzed to determine the depths of the flaws from the front surface of the CFCC material. Experimental results on carbon/carbon and CFCC samples are presented and discussed.

INTRODUCTION

Advanced ceramics, such as continuous fiber ceramic composites (CFCCs), are becoming increasingly popular. The extended use of these materials in high-temperature applications is due to their high strength-to-weight ratio and resistance to chemical reaction. These materials, however, are difficult and costly to manufacture. For these reasons, quality assurance is critical to system performance and product cost reduction. Nondestructive evaluation (NDE) has become an integral part of testing the ceramic components.

One of the most important tasks of NDE is the detection and characterization of internal flaws. The type of flaw most critical to the application of the CFCC materials is delamination which causes lifetime reduction and often occurs in CFCC materials. To advance the area of flaw characterization in CFCCs, we have developed a method to determine flaw depth below the surface using a front-flash thermal imaging system developed at Argonne National Laboratory (ANL). Front-flashing NDE examines the variation of the surface temperature of a sample after a single thermal pulse has been applied to that surface. A highly sensitive, high-speed infrared camera and locally written software were utilized to measure and analyze the surface temperature/time relationship (known as the cooling curve) on the sample's surface. In this study, flat-bottom holes machined at the back surface of flat CFCC specimens were used to simulate delamination flaws. By comparing the cooling curves over a flawed region and a homogeneous area of the material, we were able to correlate the NDE data with the depth of the flaw below the front surface of the material.

EXPERIMENTAL SETUP

The thermal imaging system developed at ANL consists of an infrared camera with a 256 x 256 focal-plane array of InSb detectors, a 200 MHz Pentium-based PC computer equipped with a

DISCLAIMER

high-speed digital frame grabber, and a function generator that produces an adjustable frame rate for the camera. The thermal pulse is applied with a photographic flash lamp system. A dual-timing trigger is used for simultaneous triggering of the flash lamps and data acquisition. An analog video system is used to monitor the experiments.

In setting up for the front-flash measurement, the lamps are placed on the same side of the sample as the camera (see Fig. 1). When the lamps are triggered, the computer simultaneously begins acquiring a series of thermal images from the infrared camera at a preset rate. These thermal images represent the surface temperature decay as a function of time (i.e., the cooling curves) over the entire region of the viewed surface. The computer then stores the digital images on a hard disk for further processing.

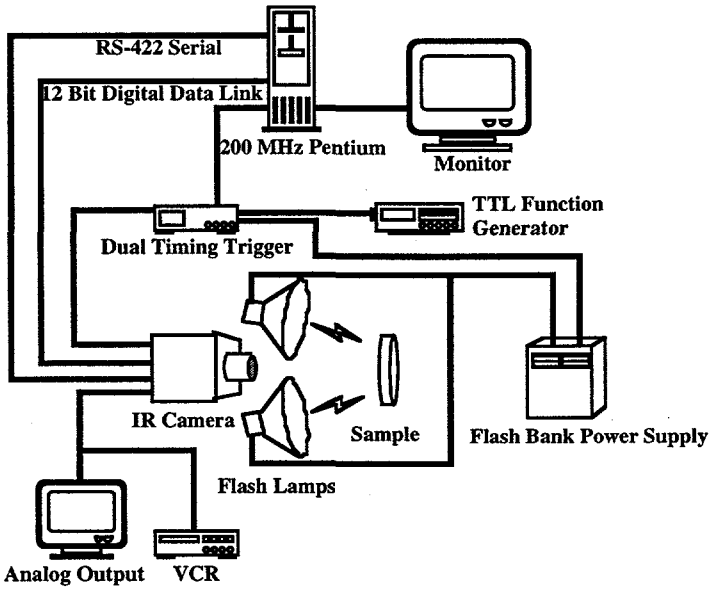

Fig. 1. Schematic diagram of thermal imaging system in front-flash setup.

DETERMINATION OF FLAW DEPTH FROM FRONT-FLASH DATA

Variation of a sample's surface temperature after a pulse of thermal energy has been applied may show some indication of internal flaws. These flaws usually have different thermal properties than the rest of the material. For instance, an internal delamination filled with air will have reduced thermal conductivity; the difference in thermal properties influences the heat flux (produced from the thermal pulse) in the material and therefore the surface temperature of the sample. The temperature decay of the heated surface is then indicative of the nature of the underlying material. It can be shown that the cooling curve over a flawed region will decay at a slower rate than that over a homogeneous section of the material. As a result, local "hot spots" appears on the front surface at regions with internal flaws. The times when these spots appear depend on the depths of the flaws, i.e., a shallow flaw appears earlier while a deeper flaw appears later.

The depth of the flaw beneath the surface can be determined by subtracting the cooling curve over an unflawed region from the cooling curve over a flawed region. The resulting curve is known as the temperature-difference curve (or contrast curve). Favro et al. (1995) suggested a relationship between the depth of the flaw and two characteristic points on the temperature-difference curve. These points are the peak difference and the peak slope on the temperature-difference curve (see Fig. 2). The corresponding times when these characteristic points occur are

indicated as peak difference time and peak slope time, respectively, in Fig. 2, and can be used to correlate the depth of the flaw.

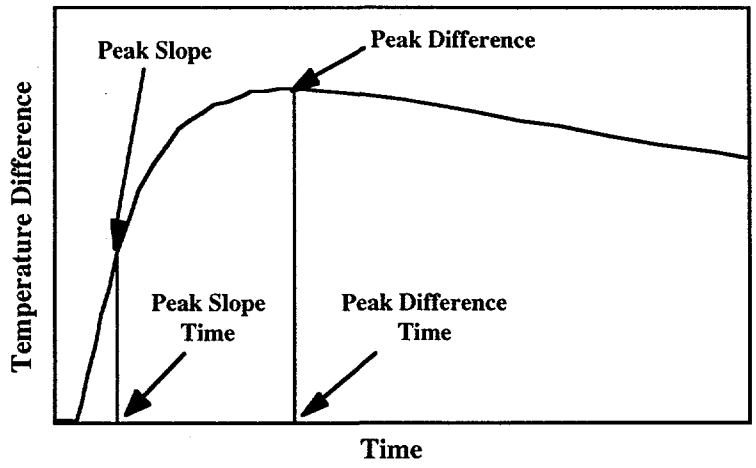

Fig. 2. Temperature-difference curve showing characteristic times.

RESULTS

Front-flash thermal imaging tests were conducted on three flat-plate specimens, i.e., a carbon/carbon (C/C) specimen and two CFCC specimens. These specimens were machined with flat-bottom holes of various diameters and depths at the back surface. They were used to simulate subsurface delaminations of different sizes and depths from the front surface.

C/C Specimen

This specimen is a 25-mm-thick C/C composite plate machined with six flat-bottom holes at the back surface. These holes all have the same diameter (12 mm) but different lengths. When viewed from the front surface, the depths of the hole bottoms below the front surface ranged from 0.5 to 3 mm with an increment of 0.5 mm, as illustrated in Fig. 3.

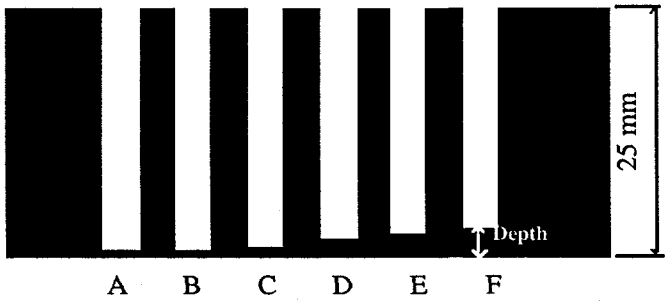

Hole	Depth (mm)
A	0.5
B	1.0
C	1.5
D	2.0
E	2.5
F	3.0

Fig. 3. Diagram of C/C specimen with six flat-bottomed holes at back surface.

Figure 4 shows an infrared thermal image (at spatial resolution of 0.3 mm/pixel) of the front surface after the thermal flash has been applied. It shows the thinnest material layer (0.5 mm) at left with the highest temperature rise and the thickest layer (3 mm) at right with the smallest temperature rise. The temperature difference for each of the six holes was determined by subtracting the average temperature over the flawed area from that of two adjacent areas with no subsurface flaws. Use of two (rather than one) unflawed areas may reduce the effect of nonuniform heating. The corresponding difference curves as a function of time for the six holes

are plotted in Fig. 5. It is seen that the temperature difference may reach 2.3°C for the thinnest flaw at 0.5 mm, and the temperature difference is ≈0.2°C for the thickest flaw at 3 mm from the surface.

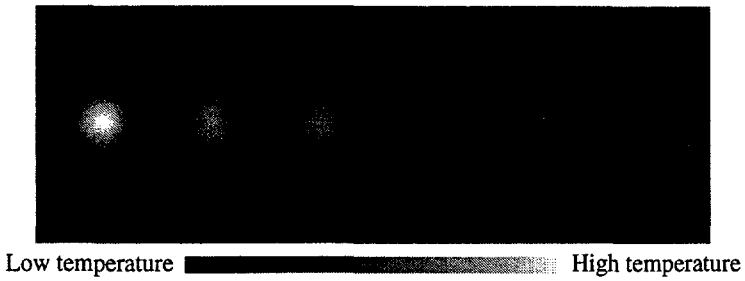

Fig. 4. Thermal image on front surface of C/C specimen after flash.

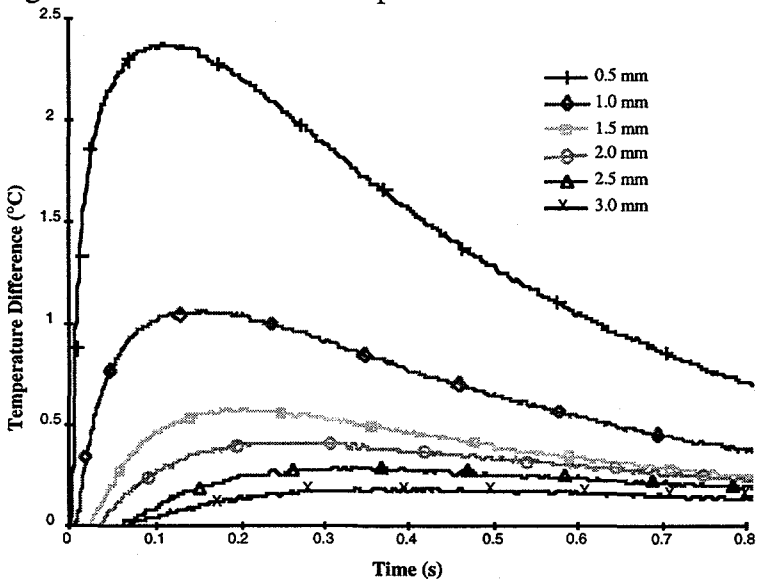

Fig. 5. Temperature difference curves for six flaws in C/C sample.

The peak-difference time and peak-slope time can be determined from Fig. 5 for each flaw. These characteristic times are plotted in Fig. 6 with respect to the squared depth of the flaws. It is evident that both the peak-difference and peak-slope times are linear functions of the squared depth, as indicated by the fitted lines in Fig. 6. The peak-slope time approaches zero as the depth reaches zero. However, the peak-difference time approaches a nonzero value as depth diminishes. Analytical methods should be used to study these phenomena at shallow depths because experimental work becomes very difficult under these limiting conditions.

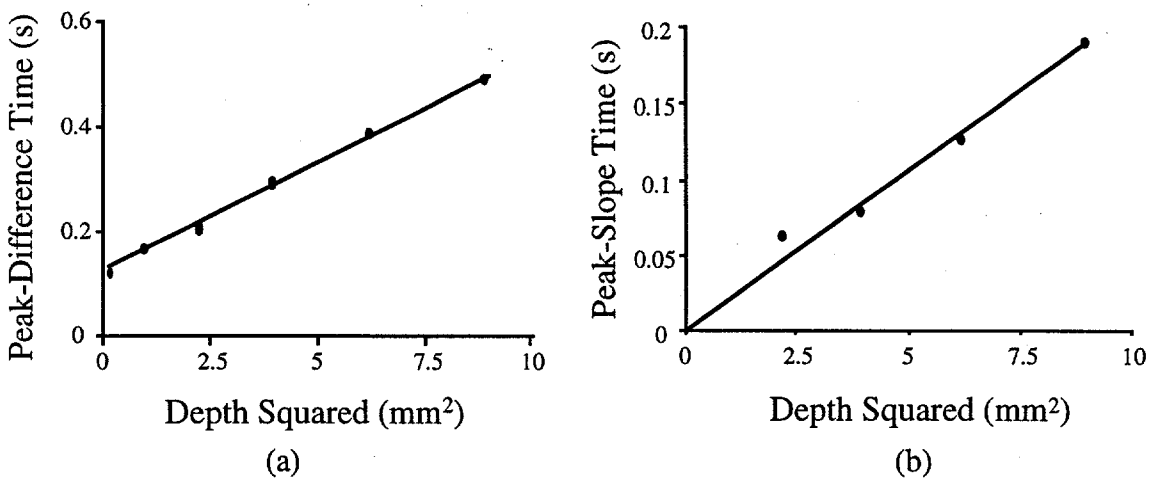

Fig. 6. Plots of (a) peak-difference time and (b) peak-slope time vs. squared depths of the six flaws in C/C sample.

CFCC Specimens

Two SiC/SiC CFCC flat plates were used in this study. The first plate was fabricated by Dow Corning Corporation (DCC). It comprised of CG-Nicalon fibers woven into an 8HS fabric and processed with polymer impregnation and pyrolysis (Easler et al., 1997). The second plate was made by DuPont Lanxide Composites, Inc (DLC). with CG-Nicalon fiber 2D plain weave in 0/45 layup and processed with chemical vapor infiltration. Figure 7 includes a schematic diagram of these two specimens with machined holes of various diameters and lengths. As indicated in the figure, the DCC specimen has all six holes while the DLC specimen contains only two usable holes due to a machining problem. Prior to machining, through-thickness thermal diffusivity was measured in each specimen with a technique developed at ANL (Stuckey et al., 1997). The results showed that both plates were relatively homogeneous, with a thermal diffusivity of 0.97 mm^2/s for the DCC specimen and 2.8 mm^2/s for the DLC specimen. These values are consistent with those obtained for similar materials by Sun et al. (1997).

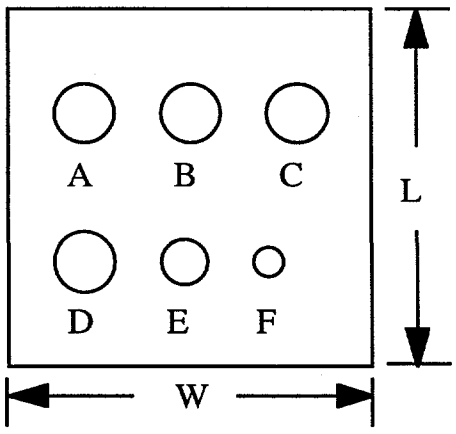

DCC Specimen

Hole	Diameter (mm)	Flaw Depth (mm)
A	7.5	0.25
B	7.5	1.12
C	7.5	0.97
D	7.5	0.87
E	5.0	0.78
F	2.5	0.85

L = 5.0 mm
W = 5.0 mm
Thickness = 2.6 mm

DLC Specimen

Hole	Diameter (mm)	Flaw Depth (mm)
A	7.5	1.38
B	n/a	
C	7.5	0.63
D	n/a	
E	n/a	
F	n/a	

L = 4.0 mm
W = 4.0 mm
Thickness = 6.3 mm

Fig. 7. Schematic illustration of two SiC/SiC CFCC specimens with machined flat-bottom holes.

Using a procedure similar to that for analyzing the C/C specimen, we determined the peak-difference and peak-slope times for each machined hole in the two CFCC specimens. These characteristic times are plotted in Fig. 8 versus the squared depths of the flaws with constant diameter of 7.5 mm. It is apparent that a linear relationship exists between both peak-difference time and peak-slope time and the squared depths of the flaws. The characteristic times for the DCC specimen are higher than those for the DLC specimen, due to the difference in thermal diffusivities of these materials. As discussed above, the DCC specimen has a lower thermal diffusivity than the DLC specimen.

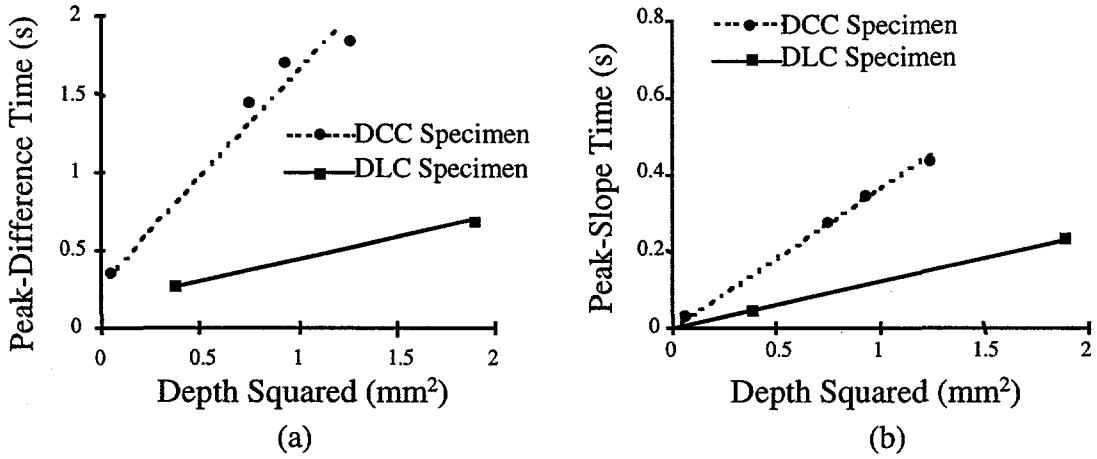

Fig. 8. (a) peak-difference time and (b) peak-slope time vs. squared flaw depth for holes with diameter of 7.5 mm.

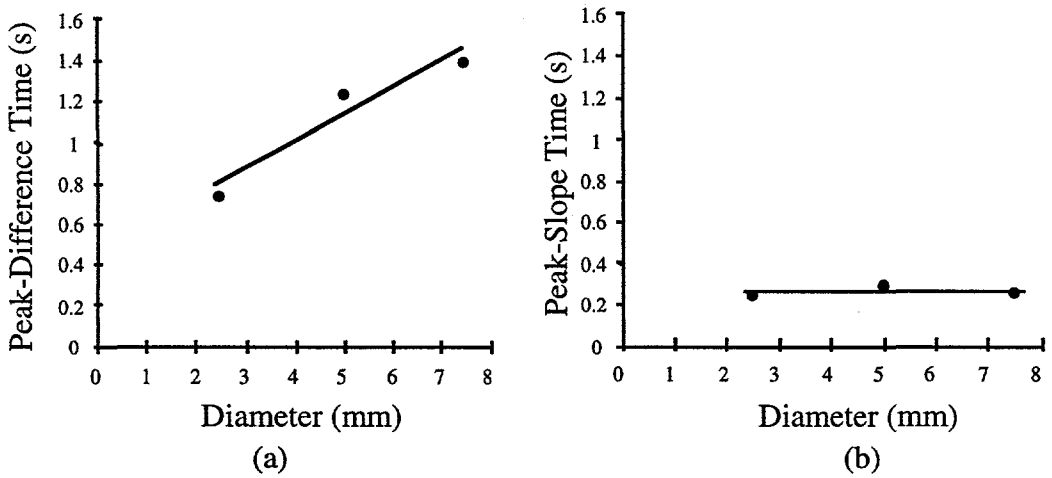

Fig. 9. (a) peak-difference time and (b) peak-slope time vs. diameter for flaw depth of 0.85 mm in DCC specimen.

Figure 9 shows the relationship between the characteristic times and the diameter of the flat-bottom holes at a flaw depth of 0.85 mm in the DCC specimen. These data shows that the diameter of the flaw has an effect on the peak-difference time. It appears that the peak-slope time remains constant with changing flaw diameter. These observation are consistent with those of Han et al. (1996).

CONCLUSIONS

This study examined the front-flash thermal imaging technique for use in the determination of flaw depth beneath the surface of CFCC materials. A high-speed, highly sensitive infrared camera was used to measure the surface temperature/time relationship. We found that the front-flash technique is capable of correlating the depth of flat-bottom holes (the flaws) to the peak-difference and the peak-slope times. Both of these characteristic times are linear functions of the squared depths of the flaws. However, peak-difference time varies with flaw diameter, whereas peak-slope time appears to remain constant with respect to the diameter.

ACKNOWLEDGMENTS

This work was funded by the U.S. Department of Energy, Energy Efficiency and Renewable Energy, Office of Industrial Technologies, under Contract W-31-109-ENG-88. The authors thank Drs. T. E. Easler and A. Szweda of Dow Corning Corporation for providing a test sample used in this study.

REFERENCES

Easler, T. E., Szweda, A., Ellingson, W. A., Sun, J. G., and T. A. K. Pillai, 1997, Characterization of Macrostructure Development in SYLRAMIC™ Ceramic Matrix Composites Using NDE Techniques, submitted for publication in J. Composite Materials.

Favro, L. D., Han, X., Wang, Y., Kou, P. K., and Thomas, R. L., 1995, Pulse-Echo Thermal Wave Imaging, in Review of Progress in QNDE, Vol. 14, Plenum Press.

Han, X., Favro, L. D., Kou, P. K., and Thomas, R. L., 1996, Early-Time Pulse-Echo Thermal Wave Imaging, in Review of Progress in QNDE, Vol. 15, Plenum Press.

Stuckey, J., Sun, J. G., and Ellingson, W. A., 1997, Rapid infrared characterization of thermal diffusivity in continuous fiber ceramic composite components, presented at 8th Int. Symp. on Nondestructive Characterization of Materials, Boulder, CO, June 15-20.

Sun, J. G., Deemer, C., Ellingson, W. A., Easler, T. E., Szweda, A., and Craig, P. A., 1997, "Thermal imaging measurement and correlation of thermal diffusivity in continuous fiber ceramic composites," in Thermal Conductivity 24, Eds. P. S. Gaal and D. E. Apostolescu, pp. 616-622, 1999, and presented at 24th Int. Thermal Conductivity Conf., Pittsburgh, Oct. 26-29, 1997.